Deembedding the Effect of a Local Ground Plane in Electromagnetic Analysis

James C. Rautio, *Fellow, IEEE*

***Abstract*—In electromagnetic analysis of complex planar circuits, it may be necessary to use internal ports, e.g., in locations where surface mount devices might later be attached. These internal ports require a local ground plane for ground reference when access to the global ground reference is unavailable. Even if perfectly conducting, use of such a ground plane still introduces excess phase in the local ground currents. This paper describes how to remove the effect of a lossy or lossless local ground, even including multiple closely spaced ports.**

***Index Terms*—Calibration, deembedding, electromagnetic analysis, imperfect ground, low-temperature co-fired ceramic (LTCC), planar circuit, surface mount device (SMD), surface mount technology (SMT).**

I. Introduction

MOST high-frequency and microwave circuit analysis makes use of ports and nodes. A port is two terminals, one terminal arbitrarily designated as the "signal," the other arbitrarily assigned to be the "ground." The port voltage is the difference in voltage between the two terminals. There is no inherent requirement that any one ground terminal be at the same potential as any other ground terminal.

The concept of a node is used in nodal analysis. The voltage of each node in a circuit is referenced to a single common global ground. Nodal analysis is commonly used to analyze interconnected systems of N-port devices. This is possible when all port ground terminals are connected to the same global ground. Thus, the port voltage is identical to the node voltage in nodal analysis. This allows N-port devices to be freely incorporated into a nodal analysis of the complete system. It is upon this principle that modern high-frequency and microwave circuit analysis is based.

However, due to the increased complexity of microwave circuitry, access to, or even the existence of a global ground cannot be assured. For example, surface mount devices (SMDs) [also known as surface mount technology (SMT)] are in common use on multilayer planar circuits including low-temperature co-fired ceramic (LTCC). With 12 or more layers, the top surface of an LTCC circuit is a considerable distance from any ground plane that might exist at the bottom. The SMD components mounted on the top surface do not have (and do not require) access to the global circuit ground.

Manuscript received April 14, 2004; revised June 20, 2004.

The author is with Sonnet Software Inc., North Syracuse, NY 13212 USA (e-mail: rautio@sonnetsoftware.com).

Digital Object Identifier 10.1109/TMTT.2004.840576

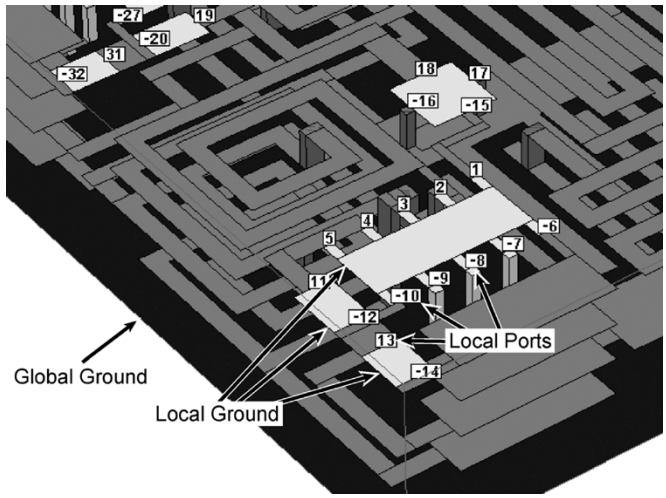

Fig. 1. Advanced LTCC circuit with topside internal ports for numerous SMDs.

Fig. 1 shows an example LTCC circuit. The light top-side metal represents attachment pads for numerous SMD components. Several of the SMD local grounds and local ports are indicated. The complex interconnections beneath the local grounds do not allow access to the global ground.

The result of electromagnetic analysis is an N-port device (usually scattering, or S-parameters as a function of frequency). As in the LTCC example above, the SMD themselves are typically not included in the electromagnetic analysis. Rather, internal ports are located at the SMD pin locations so that modeled or measured data for the SMD can be connected into the LTCC circuit later using nodal analysis.

The problem is that these internal ports have no access to global ground, but nodal analysis requires all nodes to be referenced to global ground. A partial solution is to provide the SMD internal ports with a local ground and then to prohibit any later nodal analysis connections between any nodes referencing different grounds, global or local. Connections may be made between nodes referencing the same local ground, and between any nodes referencing global ground, but not between local and global ground referenced nodes. In fact, assigning one ground to be local and another to be global is itself arbitrary. In reality, all grounds are local.

Even a perfectly conducting ground introduces delay in the ground return current. This delay, and loss if present, modifies the N-port S-parameters. If one has access only to the N-port current and voltage information, there is no way to differentiate between the effect of the ground and signal current paths.

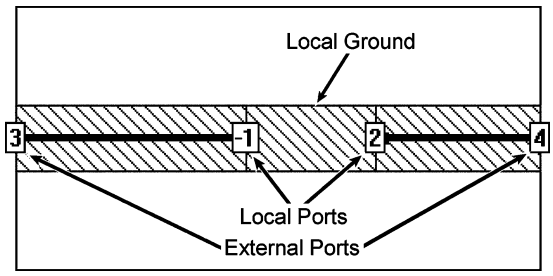

Fig. 2. Local ground deembedding standard for two local ports includes transmission lines connecting the local ports to the box sidewalls. The box sidewall ports are then deembedded and their reference planes shifted to their mating local ports. A negative number on an internal port indicates positive current flows to the left.

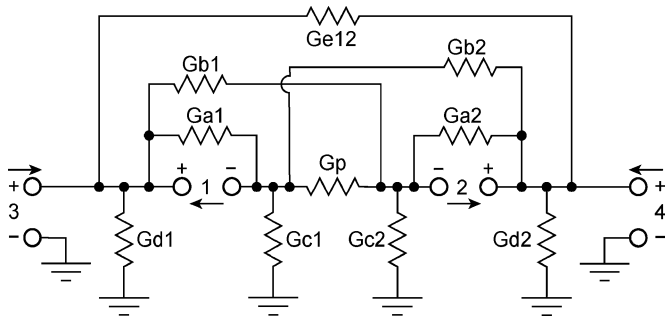

Fig. 3. Equivalent circuit of the two-port local ground deembedding calibration standard shows the local ports 1 and 2 polarized so that positive current flows out of the local ground G_p. Ports 3 and 4 are sidewall (external) ports and are polarized so positive current flows out of the sidewall (global) ground.

From the viewpoint of the N-port data, either the arbitrarily assigned ground or signal path can be considered lossless and delay free, with all the S-parameters determined by the other path, and exactly the same S-parameters result.

The reality that the ground current experiences delay, and may have loss, is not of concern for nodal analysis, as long as the voltage difference between different ground terminals is of no consequence, as in a cascade of lossy transmission lines.

When measuring an SMD, the effect of the actual ground current delay and loss is included in the SMD N-port data. When using a local ground in electromagnetic analysis, the effect of the local ground current is also included. Since the SMD measurement already includes the effect of the actual ground, we must identify and remove the additional effect of the local electromagnetic analysis ground if we are to achieve an accurate analysis.

In addition to the effect of the local ground, there are also fringing fields surrounding each SMD port and fringing field coupling between each port. Since the SMD measurement already includes the actual port discontinuities, the complete coupled N-port discontinuity present in the electromagnetic analysis must be removed.

Finally, there is coupling between the local electromagnetic analysis ground and the global ground. Since the actual SMD-to-global ground coupling is already included in the SMD measurement, the electromagnetic local-to-global ground coupling must be removed as well.

Exactly characterizing and removing the entire effect of the local ground is the topic of this paper. We refer to this deembedding algorithm as general local ground (GLG) deembedding.

II. Local Ground Calibration Standard

The electromagnetic analysis used in this study [1], [2] makes use of a "double delay" [3] deembedding algorithm for sidewall ports (ports 3 and 4 in Figs. 2 and 3). The double delay is the first application of modern microwave measurement calibration techniques [4] to electromagnetic analysis. The double-delay algorithm is closely related [5], [6] to the short-open-calibration (SOC) deembedding algorithm [7], [8]. This type of deembedding uses a perfect ground (real or virtual) for establishing a perfect (to within the numerical precision used) ground reference for sidewall ports. The deembedding additionally (and optionally) transfers the perfect ground reference to the interior of the box along a uniform port connecting transmission line by shifting the reference plane. Establishing this perfect ground reference at the local ports of the GLG calibration standard (ports 1 and 2 in Fig. 2) is critical in achieving full accuracy for the complete GLG deembedding. For this first tier deembedding, only algorithms such as SOC and double delay, which use a perfect ground reference, are recommended.

The circuit for the local ground calibration standard (Fig. 2 and 3) shows the deembedded sidewall ports (3 and 4) shifted up to the local ports (1 and 2). There is zero impedance between the signal terminal of each sidewall port and its mating local ground port. The sidewall port ground terminal is connected to global ground. The local port ground terminal is connected to the local ground.

Notice that the local ports (1 and 2) cannot be treated as single nodes. If this circuit is to be analyzed with nodal analysis, six nodes are required. Unfortunately, the full six-node information is not available. The electromagnetic analysis provides information only about the difference in voltage between the two terminals of a local port; we do not know the voltage between each terminal and global ground.

The direction of positive current for the local ports in circuit theory (Fig. 3) is away from the local ground (G_p), as indicated. In contrast, the direction of positive current in an electromagnetic analysis depends on the physical direction. In Fig. 2, the electromagnetic analysis has positive current flowing to the right. In Fig. 3, port 2 has positive current also flowing to the right, so there is no problem. However, port 1 (in Fig. 3) must have positive current flowing to the left. To change the direction of positive current for port 1 in the electromagnetic analysis to match circuit theory, we just change the sign of the port to -1. This makes the positive current direction for both the circuit of Fig. 3 and the electromagnetic analysis of Fig. 2 the same. If this is not done, then transmission S-parameters are shifted in phase by 180°. For this electromagnetic analysis, as displayed in Fig. 2, all ports on the left and top sides of a local ground must have their sign changed.

The Y-parameters of any N-port are determined by placing a voltage source on one port, short-circuiting all other ports, and evaluating the resulting current. This can be done even when some of the ground terminals are not connected to global

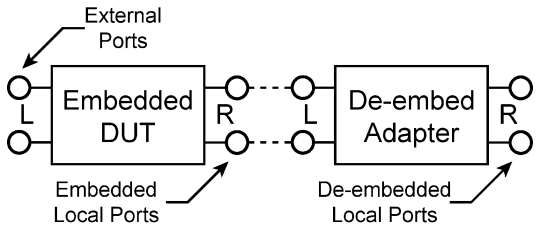

Fig. 4. For direct deembedding, the cascading parameters of the embedded DUT are multiplied by the deembedding adapter cascading parameters, thus deembedding the embedded DUT.

ground. For the circuit of Fig. 3, the Y-parameters are shown in (1) at the bottom of this page.

The Y-parameters for more than two local ports are straightforward with some of the terms in (1) becoming sums. The schematic and (1) are for real conductances to simplify presentation. In general, all terms are complex. We use the symbol G to indicate lumped elements and Y to indicate matrix elements.

With knowledge that the signal path for this circuit is lossless and delay free (i.e., the signal terminals of ports 1 and 3 are shorted together, and ports 2 and 4 as well), we conclude that all the N-port data is due to the local ground.

We can consider G_p to be the local ground, G_a to be the self-fringing fields of each port, G_b and G_e to be the port-to-port fringing field coupling, G_c to be the local port ground terminal and local ground body to global ground coupling, and G_d to be the port signal terminal coupling to global ground. Linear combinations of the Y-parameters of (1) uniquely determine all of the elements in Fig. 3. Thus, the local ground is characterized.

III. Direct Local Ground deembedding

Once the discontinuity to be deembedded is characterized, it can usually be removed by converting to cascading (e.g., $ABCD$) parameters and inverting. This yields the "deembedding adapter." The deembedding adapter cascading matrix is multiplied by the cascading matrix of the device-under-test (DUT). In this case, the circuit to be deembedded, as in Fig. 4.

Cascading matrices must be square and have an even number of ports. In the illustrated case, for one local port, the deembedding adapter has two ports and, thus, a 2×2 cascading matrix. However, the DUT can have any number of ports, one or more. In addition, the DUT may have an odd number of ports. Thus, it might appear that we cannot use cascading matrices to connect the deembedding adapter to the embedded DUT.

We might be tempted to calculate the deembedding adapter and then somehow apply nodal analysis to connect it to the DUT. This is impossible because, as mentioned above, nodal analysis assumes the voltage of each node is referenced to global ground. We do not have this information for the local ports.

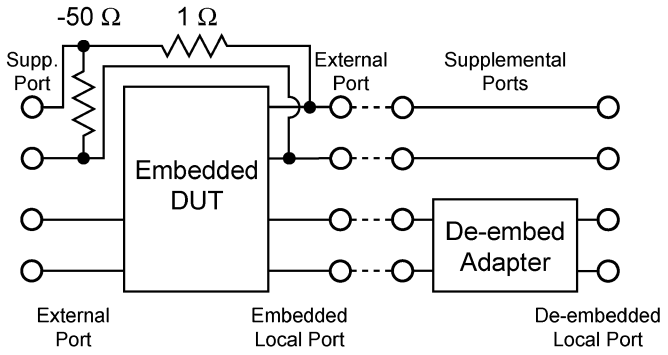

Fig. 5. Both the embedded DUT and deembedding adapter have supplemental ports added to allow any number of DUT ports. The DUT supplemental ports are effectively open circuited when S-parameters are calculated.

Thus, we return to cascading matrices. If we modify both the embedded DUT and the deembedding adapter, we can form two square matrices with an even and equal number of ports.

This is done by adding supplemental ports to both the embedded DUT and the deembedding adapter as needed (Fig. 5). Ports are added to the DUT by using nodal analysis to connect a resistor (any nonzero value, 1 Ω shown) from an existing port to the added supplemental port. A −50-Ω resistor is then added from the supplemental port to ground. After deembedding and conversion to S-parameters, the −50-Ω resistor combines with the 50-Ω resistor terminating the supplemental port in the S-parameter definition. This leaves the supplemental port open so that it has no effect on the other S-parameters.

When the number of external ports is less than the number of local ports, then supplemental DUT ports must be connected to one or more local ports. Supplemental ports so created by nodal analysis are also local ports, and no special nodal analysis consideration is needed.

The deembedding adapter is supplemented by adding through connections until the required number of ports is realized. After the matrices are multiplied, all DUT supplemental ports are ignored, and the effect of the local ground is removed from the DUT.

It would seem the deembedding algorithm is complete, except for one final problem. If the local ground is floating, and G_c of Fig. 3 become small (typically at low frequency), then the cascading parameters become poorly conditioned. A simple solution for this problem is to require some kind of physical attachment from local ground to global ground. The attachment can be minimal, high resistance and reactance, as long as it keeps G_c from going to zero.

The fact that a nonsingular solution exists is seen by noticing that the Y-parameters corresponding to the inverted cascading parameters are those of (1) with a sign change. With this change,

$$\underline{\underline{Y}} = \begin{bmatrix} G_p+G_{a1}+G_{c1}+G_{b2} & -G_p & -(G_p+G_{c1}+G_{b2}) & G_p+G_{b2} \\ -G_p & G_p+G_{a2}+G_{c2}+G_{b1} & G_p+G_{b1} & -(G_p+G_{c2}+G_{b1}) \\ -(G_p+G_{c1}+G_{b2}) & G_p+G_{b1} & G_p+G_{b1}+G_{c1}+G_{d1}+G_{b2}+G_{e12} & -(G_p+G_{b1}+G_{b2}+G_{e12}) \\ G_p+G_{b2} & -(G_p+G_{c2}+G_{b1}) & -(G_p+G_{b1}+G_{b2}+G_{e12}) & G_p+G_{b2}+G_{c2}+G_{d2}+G_{b1}+G_{e12} \end{bmatrix} \quad (1)$$

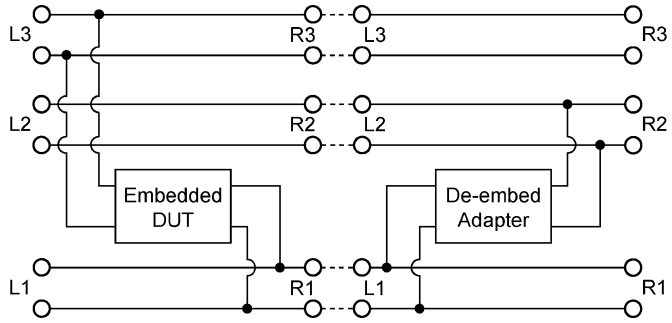

Fig. 6. By connecting both the embedded DUT and the deembedding adapter in a double-port configuration, the overall cascading matrices become well conditioned even when the local ground and global ground are completely isolated.

all the positive conductances of Fig. 3 become negative. When the circuit of Fig. 3 is cascaded with a mirror image of itself, with all the conductors negative, it is seen that the local ground is not reduced to a perfect short circuit. Rather, the local ground becomes an open circuit and is completely removed from the circuit. The perfect zero-delay zero-loss signal path of the deembedding adapter takes its place. At least graphically, we see that zero G_c does not cause any fundamental problem. A solution must exist that does not involve singularities.

IV. Double-Port deembedding

To avoid poorly conditioned cascading matrices, we connect the embedded DUT and the deembedding adapter in a double port configuration (see Fig. 6).

Each port of the original N-port is connected to two ports, one on either side. In Fig. 6, each of the six labeled ports are drawn as single ports. In general, each illustrated port represents multiple ports. The number of $L1$–$R1$ ports is equal to the number of local ports. The number of $L2$–$R2$ ports is also equal to the number of local ports. The number of $L3$–$R3$ ports is the number of external DUT ports (i.e., all DUT ports, except local ports).

The total number of ports is twice the number of DUT ports plus twice the number of local ports. After cascading, all ports, except $R2$ and $R3$ are terminated in open circuits. Ports $R2$ and $R3$ then represent the deembedded DUT.

If $ABCD$ cascading parameters are used, conversion to S-parameters is usually realized by converting first to Y- or Z-parameters. However, a common test is to deembed the calibration standard. In this case, there are open circuits between local ports. This results in undefined Z-parameters. There are also short circuits between the sidewall and deembedded local ports. This results in undefined Y-parameters.

In order to successfully deembed the standard, the $ABCD$-parameters can first be converted from current/voltage to incident/reflected waves, and then to S-parameters. Y- or Z-parameters cannot be intermediate results.

Rather than convert to wave variables after cascading, we work with wave variables throughout. The wave-variable equivalent of the cascading matrix is R-parameters [9] as follows:

$$\begin{bmatrix} b_1 \\ a_1 \end{bmatrix} = \begin{bmatrix} R_{11} & R_{12} \\ R_{21} & R_{22} \end{bmatrix} \begin{bmatrix} a_2 \\ b_2 \end{bmatrix} \tag{2}$$

where a_i are incident wave amplitudes and b_i are reflected wave amplitudes. For more than two ports, a_i and b_i become vectors and R_{ij} become matrices. Conversion from S-parameters is

$$\underline{\underline{R}} = \begin{bmatrix} S_{12} - S_{11}S_{21}^{-1}S_{22} & S_{11}S_{21}^{-1} \\ -S_{21}^{-1}S_{22} & S_{21}^{-1} \end{bmatrix}. \tag{3}$$

This conversion is more easily realized for N ports by first swapping the right $N/2$ columns with the left $N/2$ columns. Then perform a partial matrix inversion, solving only the last $N/2$ rows. Gaussian elimination routines are easily modified to do a partial solve. Such routines usually have an integer array that keeps track of which rows have been solved. To solve the last $N/2$ rows only, initialize that array to indicate that the first $N/2$ rows have already been solved. To convert from R- back to S-parameters, reverse the steps. Do a partial solve on the last $N/2$ rows, and then swap columns. Alternatively,

$$\underline{\underline{S}} = \begin{bmatrix} -R_{11}^{-1}R_{12} & R_{11}^{-1} \\ R_{22} - R_{21}R_{11}^{-1}R_{12} & R_{21}R_{11}^{-1} \end{bmatrix}. \tag{4}$$

In order to insert the deembedding adapter into the double-port connection of Fig. 6, we must first determine the S-parameters of the deembedding adapter. Normally, one would convert the S-parameters of the calibration standard to cascading parameters, invert the cascading parameter matrix, then convert back to S-parameters. However, we cannot use cascading parameters (neither R, nor $ABCD$) for this task due to the problems with poor conditioning when G_c of Fig. 3 becomes small.

Prior to deembedding, the Y-parameters of the calibration standard still exist. Thus, we convert to Y-parameters and then change the sign of each Y-parameter. We then convert back to S-parameters. This process converts the S-parameters of the calibration standard into the S-parameters of the deembedding adapter without using cascading parameters.

The S-parameters for the deembedding adapter inserted into the double-port connection on the right-hand side of Fig. 6 are

$$\begin{bmatrix} b_{L1} \\ b_{L2} \\ b_{L3} \\ b_{R1} \\ b_{R2} \\ b_{R3} \end{bmatrix} = \begin{bmatrix} S'_{11} & S'_{12} & 0 & 1+S'_{11} & S'_{12} & 0 \\ S'_{21} & S'_{22} & 0 & S'_{21} & 1+S'_{22} & 0 \\ 0 & 0 & 0 & 0 & 0 & 1 \\ 1+S'_{11} & S'_{12} & 0 & S'_{11} & S'_{12} & 0 \\ S'_{21} & 1+S'_{22} & 0 & S'_{21} & S'_{22} & 0 \\ 0 & 0 & 1 & 0 & 0 & 0 \end{bmatrix} \begin{bmatrix} a_{L1} \\ a_{L2} \\ a_{L3} \\ a_{R1} \\ a_{R2} \\ a_{R3} \end{bmatrix}. \tag{5}$$

As in Fig. 6, each of the indicated ports may actually represent multiple ports, making each matrix element above into matrices themselves.

S'_{ij} are the S-parameters of the deembedding adapter with an additional 50-Ω resistor connected from each port to ground [see Fig. 7(a)]. This provides all the S-parameters in (5), except the terms like $1 + S'_{ii}$.

One such term is $S_{R1,L1}$. This term is determined by a source on port $L1$ generating a wave exiting port $R1$ with all ports terminated in 50 Ω. The deembedding adapter places a shunt admittance across the $L1$–$R1$ through line, as shown in Fig. 7(b).

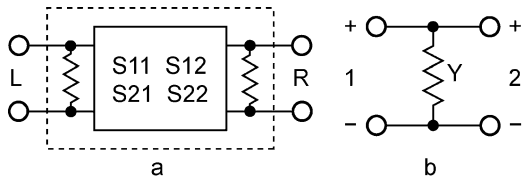

Fig. 7. Adding shunt 50-Ω resistors to each port of the deembedding adapter: (a) allows calculation of most of the double-port S-parameters. The remaining S-parameters require consideration of the S-parameters of (b).

Given the shunt admittance (which, in general, is a matrix) Y, we are interested in S_{21} of the circuit of Fig. 7(b) as follows:

$$S_{21} = \frac{2}{(Y+2)}. \tag{6}$$

The shunt admittance is the input admittance of the two-port of Fig. 7(a) with the extra 50-Ω resistor on the input removed as follows:

$$Y = \frac{1 - S'_{11}}{1 + S'_{11}} - 1. \tag{7}$$

Substitution of (7) into (6) yields the desired S-parameter for (5). These $1 + S'_{ii}$ terms cause the double-port connected deembedding adapter cascading matrix to be well conditioned even when the deembedding adapter cascading matrix itself is not.

In a similar manner, the DUT is inserted into a double-port connection, as shown in the left-hand side of Fig. 6. The only difference is that the external port related S-parameters are in the third and sixth rows and columns. The second and fifth row/columns are filled with zero and unit matrices.

Once the double-port DUT and deembedding adapter S-parameters are complete, they are both converted to R-parameters by (2) and multiplied in either order. The result is then converted back to S-parameters by (4). Finally, all ports, except $R2$ and $R3$, are terminated in open circuits. If we order and partition the resulting matrix so that all the $R2$ and $R3$ ports are together in the last row/columns in the matrix (S^A_{22}), we have the deembedded DUT as

$$S^{\mathrm{DUT}} = S^A_{21}\left(1 - S^A_{11}\right)^{-1} S^A_{12} + S^A_{22} \tag{8}$$

where S^A_{ij} is one component of the partitioned double-port matrix, and S^{DUT} is the desired deembedded DUT.

V. Validation

As mentioned above, an easy initial test is to deembed the calibration standard. The double-port deembedding yields a zero-loss zero-delay (to within numerical precision) multiport through in all cases tried.

The next test is to use as a DUT the calibration standard modified by setting the sidewall port reference planes to zero length. With this modification, the DUT now includes the transmission lines connecting the sidewall ports to the local ports. This allows us to deembed a DUT different from the calibration standard, providing a more rigorous validation.

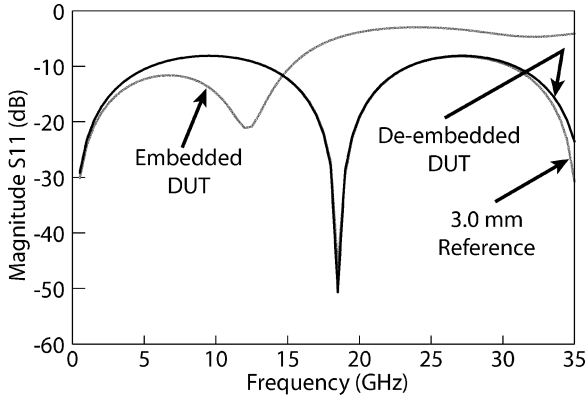

Fig. 8. Deembedded DUT compares well with a reference 3.0-mm-long line. The comparison with the embedded DUT shows the effect of deembedding the local ground.

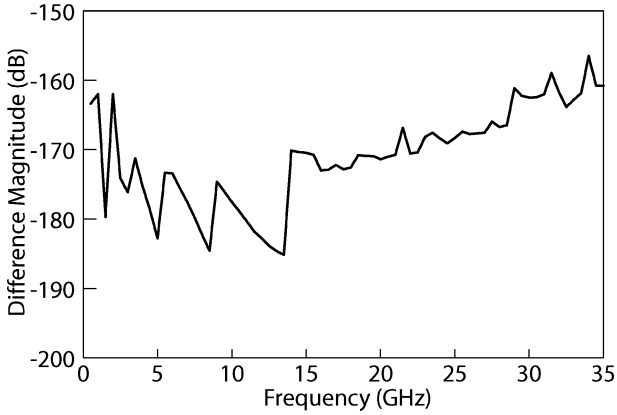

Fig. 9. In spite of using a lossless local ground in one case and a 10-kΩ per square local ground in another case, deembedding the local ground yields S-parameters that are identical to within the noise floor of the underlying electromagnetic analysis.

For this type of validation, we use the calibration standard of Fig. 2. The transmission line is 0.5-mm wide, the port 1 connecting line (left side) is 1.75-mm long, the port 2 connecting line is 1.25-mm long, and the local ground (near the center) is 1.0-mm long. The substrate has a relative dielectric constant of 10.0 and is 0.25-mm thick. There are 25 mm of air above the substrate. The box is 4.0 × 2.0 mm and is divided into 64 cells along its length and 32 cells across its width. The circuit is lossless.

The DUT is the same as the calibration standard, except the reference planes are set to zero length. After deembedding, the local ports are shorted together using nodal analysis. The results (Fig. 8) are compared to an electromagnetic analysis of a similar line with the local ground removed; the line is 3.0-mm long. There is some difference at the high end of the frequency range; this is due to the difference in box length in the DUT and the reference circuit. To show the effect of deembedding, the embedded DUT with local ports shorted together is also shown.

To provide an exact test of validity, we analyze this same DUT for two different local grounds. The first local ground is as above and is lossless. The second has only the local ground resistivity changed from 0 to 10 kΩ per square. While this is a radically different local ground, it should give the same answer after deembedding. Fig. 9 shows the magnitude

of the vector difference between the resulting S-parameters (S_{11} and S_{21} difference averaged).

In spite of the extreme difference in local grounds, the difference in S-parameters shows the noise floor of the deembedding procedure to be about the same as that of the underlying electromagnetic analysis, in this case, approximately -160 dB.

If the test of Fig. 8 is repeated using the embedded 10-kΩ local ground DUT (no GLG deembedding), an open circuit results.

VI. Failure Mechanisms

The double-port GLG deembedding fails if the first tier deembedding, removing the local-to-sidewall port connecting lines, fails. The well-understood failure mechanisms of the first tier deembedding occur when the port connecting lines allow more than one propagating mode, and when the reference plane is so short that the fringing fields from the ports at each end interact. Good microwave design avoids the first failure mode. Keeping reference planes and port connecting line lengths longer than one or two substrate thicknesses or line widths (whichever is shorter) is usually sufficient to avoid the second failure mode. In addition, the first tier deembedding fails when box resonances are excited.

The double-port GLG deembedding can tolerate very high resistance ground planes, but does fail if the ground resistance is too high. This is typically not a consideration unless the local ground is several electrically noncontacting areas. In this case, a low-frequency failure is seen as the coupling between the disjoint areas becomes small.

As mentioned above, GLG deembedding requires an essentially perfect short circuit in the calibration standard between the sidewall and local ports. To test the degree of sensitivity, we intentionally set the sidewall port reference planes back 0.0625 mm from the local ports (1/8th of a linewidth, one cell length) and repeated the deembedding using this "bad" calibration standard. The validation test of Fig. 8 was repeated. The general shape of the S_{11} curve is the same; however, the entire response is stretched up in frequency. For example, the zero at 18.5 GHz moves up over 5% to 19.5 GHz.

The GLG deembedding fails if the local ground current due to coupling with the DUT (not accounted for in the calibration standard) becomes large compared to the other local ground currents. This is not a problem for typical fringing field coupling; however, if the DUT is electrically connected to the local ground in a manner not included in the calibration standard, then the deembedding can fail. This is because the DUT has significantly changed the local ground making the calibration standard inappropriate for the DUT.

The deembedded DUT local ports are typically referenced to global ground. However, if the local ground currents induced by coupling from the DUT (not present in the calibration standard) become stronger than the local-to-global ground coupling (G_c in Fig. 3), then the DUT local ground is no longer attached to global ground. Even so, it still behaves as a perfect floating ground. If it is desired to have the local ground referenced to global ground, then one can supplement G_c with an additional physical connection to the global ground. This would be required only if it is desired to make nodal analysis connections between the local ports and any external ports, which is a rare situation.

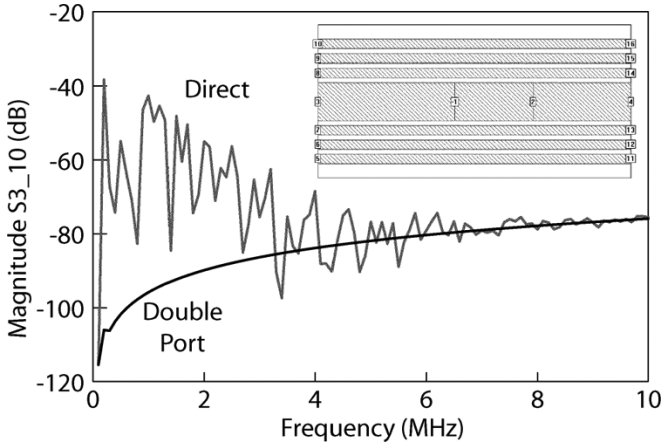

Fig. 10. Poorly conditioned cascading matrix used in the direct GLG deembedding sometimes results in noisy data, unlike the double-port GLG approach. Note the very low frequency.

As mentioned above, the direct GLG deembedding can fail when analyzing a floating ground. This is due to the poorly conditioned cascading matrix. We have not explored this problem in detail; however, we do know that the problem increases in magnitude when there are a large number of ports. It is also most prominent at low frequencies. The most peculiar aspect of the problem is that it can be clearly present in some S-parameters, but not at all in others, all in the same analysis. We have found no pattern or explanation for this.

To illustrate the problem, we modify the DUT used in the above validation tests by adding six through lines, each 0.125-mm wide, separated by 0.0625 mm, three on each side. The resulting 16-port DUT is deembedded by both the double-port GLG and the direct GLG. All the double port data and approximately 80% of the direct deembedded data are good. The rest of the direct data are noisy at low frequency. The direct data are either noisy or smooth, and there does not seem to be any kind of transition between the two states.

In Fig. 10, the same S-parameter is shown in both cases, one calculated using the double-port GLG and the other using direct deembedding. They both use the same DUT and calibration standard data. Note the low-frequency range.

Fig. 10 shows $S_{3,10}$. A similar plot of $S_{10,3}$ shows good data, further suggesting the noise is a numerical artifact of the poorly conditioned cascading matrix. It is possible that a carefully designed matrix solve and matrix multiply could reduce or eliminate the noise, especially if it is specialized to symmetric matrices. However, the preferred solution is to avoid the problem completely by using the double-port approach to GLG deembedding.

VII. Conclusion

A GLG deembedding procedure that provides complete characterization of a local ground and the removal of its effect from electromagnetic analysis data has been presented. This technique is useful when combining electromagnetic and nodal analysis for the analysis of SMDs on multilayer planar circuits.

ACKNOWLEDGMENT

The author extends special thanks to J. Merrill for suggesting the form of the calibration standard and for his patient requests over many years for a solution to this problem.

REFERENCES

[1] J. C. Rautio, "A time-harmonic electromagnetic analysis of shielded microstrip circuits," Ph.D. dissertation, Elect. Eng., Dept., Syracuse Univ., Syracuse, NY, 1986.

[2] J. C. Rautio and R. F. Harrington, "An electromagnetic time-harmonic analysis of shielded microstrip circuits," *IEEE Trans. Microw. Theory Tech.*, vol. MTT-35, no. 8, pp. 726–730, Aug. 1987.

[3] J. C. Rautio, "A de-embedding algorithm for electromagnetics," *Int. J. Microwave Millim.-Wave Computer-Aided Eng.*, vol. 1, no. 3, pp. 282–287, Jul. 1991.

[4] R. R. Pantoja, M. J. Howes, J. R. Richardson, and R. D. Pollard, "Improved calibration and measurement of the scattering parameters of microwave integrated circuits," *IEEE Trans. Microw. Theory Tech.*, vol. 37, no. 11, pp. 1675–1680, Nov. 1989.

[5] J. C. Rautio, V. I. Okhmatovski, J. Morsey, and A. C. Cangellaris, "Comments on 'On deembedding of port discontinuities in full-wave CAD models of multiport circuits'," *IEEE Trans. Microw. Theory Tech.*, vol. 52, no. 10, pp. 2448–2449, Oct. 2004.

[6] V. I. Okhmatovski, J. D. Morsey, and A. C. Cangellaris, "Authors' reply," *IEEE Trans. Microw. Theory Tech.*, vol. 52, no. 10, pp. 2449–2450, Oct. 2004.

[7] L. Zhu and K. Wu, "Unified equivalent circuit model of planar discontinuities suitable for field theory-based CAD and optimization of M(H)MICs," *IEEE Trans. Microw. Theory Tech.*, vol. 47, no. 9, pp. 1589–1602, Sep. 1999.

[8] V. I. Okhmatovski, J. Morsey, and A. C. Cangellaris, "On deembedding of port discontinuities in full-wave CAD models of multiport circuits," *IEEE Trans. Microw. Theory Tech.*, vol. 51, no. 12, pp. 2355–2365, Dec. 2003.

[9] D. M. Kerns and R. W. Beatty, *Basic Theory of Waveguide Junctions and Introductory Microwave Network Analysis*. New York: Pergamon, 1967.

James C. Rautio (S'77–M'78–SM'91–F'00) received the B.S.E.E. degree from Cornell University, Ithaca, NY, in 1978, the M.S. degree in systems engineering from the University of Pennsylvania, Philadelphia, in 1982, and the Ph.D. degree in electrical engineering from Syracuse University, Syracuse, NY, in 1986.

From 1978 to 1986, he was with General Electric, initially with the Valley Forge Space Division, then with the Syracuse Electronics Laboratory. During this time, he developed microwave design and measurement software and designed microwave circuits on alumina and on GaAs. From 1986 to 1988, he was a Visiting Professor with Syracuse University and Cornell University. In 1988, he joined Sonnet Software, Liverpool, NY, full time, a company he had founded in 1983. In 1995, Sonnet Software was listed on the Inc. 500 list of the fastest growing privately held U.S. companies, the first microwave software company ever to be so listed. Today, Sonnet Software is the leading vendor of three-dimensional planar high-frequency electromagnetic analysis software.

Dr. Rautio was the recipient of the 2001 IEEE Microwave Theory and Techniques Society (IEEE MTT-S) Microwave Application Award.